

## Optical study of structural phase transition in organic charge-transfer crystals K- and Rb-tetracyanoquinodimethane

H. Okamoto, Y. Tokura,\* and T. Koda

*Department of Applied Physics, University of Tokyo, Bunkyo-ku, Tokyo 113, Japan*

(Received 13 January 1987)

Polarized reflectivity spectra have been measured on K- and Rb-tetracyanoquinodimethane single crystals over a wide temperature range covering respective structural phase-transition temperatures. From an analysis of the intramolecular vibration spectra and charge-transfer exciton bands, thermal variations of dimeric molecular displacements at the phase transition are investigated. The temperature-dependent intensity and width of the dimerization-induced intramolecular  $a_g$  vibration bands can provide microscopic information, which is complementary to the x-ray data, on the structure change at the phase transition.

### I. INTRODUCTION

Among a number of organic charge-transfer (CT) compounds, the family of segregated-stack CT compounds of the radical anion tetracyanoquinodimethane (TCNQ) has been subject to considerable investigations in this decade, primarily on their electric properties as organic synthetic metals. These CT-compound crystals are constructed from quasi-one-dimensional columns of TCNQ molecules as the electron acceptor and separately stacked columns of an electron donor ( $D$ ). The electric properties of these complexes are largely dependent on the degree of charge transfer ( $\rho$ ) between TCNQ and the donor ( $D^{+\rho}TCNQ^{-\rho}$ ). In the case of a partial charge transfer ( $\rho < 1$ ), the compounds usually exhibit either metallic or semiconducting properties depending upon whether the one-dimensional stack of TCNQ molecules is equidistant or Peierls distorted. On the other hand, in the case of a complete charge transfer ( $\rho = 1$ ), the electronic wave functions of transferred electrons are strongly localized on TCNQ molecules, giving rise to a relatively large energy gap. This is attributable to the fact that the on-site electron-electron Coulomb repulsion ( $U$ ) is fairly large compared to the transfer energy ( $t$ ) between the adjacent molecules on the stack.

The present work deals with simple alkali-metal-TCNQ salts, K-TCNQ and Rb-TCNQ, which belong to the latter category, showing a full charge transfer from the metal to TCNQ. An important feature of these alkali-metal-TCNQ compounds is the occurrence of a structural phase transition as a consequence of the strong electron-lattice interaction inherent in quasi-one-dimensional systems. In K-TCNQ and Rb-TCNQ, such phase transitions are reported to take place at 395 and 381 K, respectively.<sup>1</sup> In order to investigate the critical behaviors at these phase transitions, measurements have been made on the spin susceptibility,<sup>2,3</sup> dc conductivity,<sup>4</sup> and x-ray scattering<sup>5</sup> as a function of temperature and heats of transition.<sup>2</sup> From these results and the x-ray structure analysis,<sup>3,6</sup> it has been proved that both K-TCNQ and Rb-TCNQ crystals undergo a dimeric lattice

distortion at the phase-transition temperature  $T_c$  by the alternating elongation and shrinkage of the intermolecular spacings on the TCNQ stack. This transition is generally accepted as a spin-Peierls phase transition.<sup>7-9</sup> From measurements of magnetic susceptibility<sup>2,3</sup> as a function of temperature, it has been revealed that the magnetic susceptibilities decrease rapidly with decreasing temperature below  $T_c$ . Such a magnetic behavior is considered to be closely related to the opening of the spin-wave gap by the lattice dimerization.

Measurements have been also reported on the optical spectra of alkali-metal-TCNQ salts. In earlier studies, the electronic spectra have been mostly investigated on powder samples of K-TCNQ and Rb-TCNQ using unpolarized light. For K-TCNQ, polarized reflection spectra have been measured on single crystals at room temperature.<sup>10-12</sup> More recently, detailed measurements of polarized reflection spectra have been conducted by Yakushi *et al.* on single crystals of K-TCNQ and Rb-TCNQ at low temperature.<sup>13,14</sup> They observed that the charge-transfer band in either crystal consists of a strong main peak and a weak subsidiary peak on the high-energy side of the main peak. The latter peak has been attributed by these authors to the band edge, but this interpretation has not yet been established.

In addition to electronic spectra in the visible to near-infrared spectral region, molecular vibration spectra in the infrared region can also provide valuable information on the CT states and the structural phase transition as well. In the undistorted lattice of TCNQ salts, the molecular vibration spectra are dominated by the ungerade (odd-parity) intramolecular vibration bands which are infrared-active in the centrosymmetric lattice of undimerized TCNQ stacks. They are usually polarized in parallel to the molecular plane of TCNQ and hence are nearly perpendicular to the stacking axis. However, when the lattice is distorted by dimerization, the gerade (even-parity) intramolecular vibration modes become optically active through a coupling with the electronic CT transition,<sup>15,16</sup> as discussed later. These distortion-induced gerade bands are strongly polarized in parallel to the

stacking axis, in contrast to most of the ungerade intramolecular vibration bands, which are predominantly polarized in the perpendicular direction. As the intensities of these gerade modes are closely correlated with the amount of dimeric distortion, these modes are utilized as a microscopic probe to detect the lattice distortion. Considerable efforts have been made on the studies of specific totally symmetric intramolecular vibrations in various kinds of segregated-stack crystals<sup>17–20</sup> and mixed-stack crystals<sup>21–26</sup> at structural phase transitions.

The aim of this work is to obtain detailed spectroscopic information on the structural phase transitions in K-TCNQ and Rb-TCNQ crystals from temperature variations of totally symmetric intramolecular vibration and electronic CT bands near the respective phase transition temperatures. Polarized reflection spectra have been measured on single crystals of K-TCNQ and Rb-TCNQ in the photon-energy region of 0.25–2.0 eV as a function of temperature. By virtue of distinct polarization properties of these spectra in single crystals, their spectral shapes could be analyzed in detail in a wide temperature range from 2 to about 400 K. Based on these experimental results, characteristic natures of the structural phase transition in K-TCNQ and Rb-TCNQ crystals are elucidated.

A brief review of the crystal structures and structural phase transitions of K-TCNQ and Rb-TCNQ crystals is given in Sec. II. After a description of experimental details and results in Secs. III and IV, a detailed discussion of the interrelationship between the optical spectra and the phase transition in terms of a simplified model is given in Sec. V.

## II. CRYSTAL STRUCTURES AND PHASE TRANSITIONS IN K-TCNQ AND Rb-TCNQ

For the sake of later discussion, we shall briefly summarize below the present knowledge of crystal structures<sup>3,6</sup> and structural phase transitions<sup>5</sup> of K,Rb-TCNQ crystals.

Both K-TCNQ and Rb-TCNQ crystals have a monoclinic structure, belonging to the space group  $P2_1/n$  for K-TCNQ and  $P2_1/c$  for Rb-TCNQ. In the complexes formed by  $\text{Rb}^+$  and  $\text{TCNQ}^-$ , there are two different crystal structures, that usually called Rb-TCNQ(I) and the other, Rb-TCNQ(II). In this study we deal with only the former, and designate it simply Rb-TCNQ. In either K-TCNQ and Rb-TCNQ crystals, the molecular stacking axis is taken to be the *a* axis. There are two modifications in the crystal structure of K-TCNQ and Rb-TCNQ. For K-TCNQ crystals, full x-ray structure determinations have been performed on the low-temperature phase at 25 °C and on the high-temperature phase at 140 °C. In the low-temperature phase there are two unequal TCNQ columns (I,II), each consisting of a parallel array of dimerized TCNQ molecules. The TCNQ molecules in the columns I and II are directed perpendicular to each other. The normals to the TCNQ molecular planes are tilted from the stacking axis by about 16° for columns I and II. The plane-to-plane separations between adjacent molecules on the respective stacks are slightly different in columns I and II.

We define the parameter  $\xi = (r_1 - r_2)/(r_1 + r_2)$  to represent the dimeric displacement of TCNQ molecules along the stack axis. Here,  $r_1$  and  $r_2$  are the interdimer and intradimer molecular separations, respectively. In the high-temperature phase, we have  $\xi = 0$ , since the lattice is not dimerized and TCNQ molecules are stacked equidistantly ( $r_1 = r_2$ ). There is no distinction in this phase between columns I and II. The normals to the TCNQ molecular planes are inclined to the stacking axis by about 14°. On the other hand,  $\xi$  takes a nonzero finite value in the low-temperature phase. The dimeric displacements are not so different in columns I and II according to the x-ray data,<sup>6</sup>  $\xi$  being estimated to be about  $4.62 \times 10^{-2}$  and  $5.08 \times 10^{-2}$  for columns I and II, respectively, at 25 °C. In the dimerized phase, TCNQ molecules are displaced not only along the stacking axis but also in the lateral direction, parallel to the molecular planes.

As for Rb-TCNQ crystal, the crystal structure has been known only for the low-temperature modification at –160 °C.<sup>3</sup> In this phase there is only one kind of TCNQ column, which is also dimerized along the stacking axis. The parameter  $\xi$  is estimated to be about  $4.89 \times 10^{-2}$  at –160 °C. The molecular plane of TCNQ is considerably inclined to the stacking axis (by about 23°). The lateral displacement of adjacent TCNQ molecules belonging to the different dimers is larger in Rb-TCNQ than that of K-TCNQ in the low-temperature phase.

The temperature dependence of dimeric distortions provides key information on the nature of phase transition in K-TCNQ and Rb-TCNQ. Terauchi has investigated in detail the temperature dependence of the superlattice x-ray reflection intensities in the low-temperature phase.<sup>5</sup> The observed reflection intensities are proportional to the squared displacement ( $\xi^2$ ) of TCNQ molecules from their equilibrium positions. For reference, the results are reproduced in Fig. 1. When the temperature is raised, the intensities diminish gradually and then suddenly disappear at  $T_c$  in either crystals. But the thermal behaviors are somewhat different between K-TCNQ and Rb-TCNQ: In K-TCNQ the intensity is considerably decreased before a weak discontinuous drop occurs at  $T_c$ . This indicates that the dimeric displacement varies continuously over a fairly wide temperature range until the first-order-like jump takes place at  $T_c$ . In contrast, the displacement in Rb-TCNQ diminishes rather abruptly at  $T_c$ . Such a difference is also reflected in the thermal behaviors of the x-ray diffuse-scattering intensities above  $T_c$ .<sup>5</sup> In K-TCNQ, a remarkable increase of diffuse-scattering intensity is observed when the temperature is lowered to  $T_c$ , indicating an appreciable critical fluctuation in the lattice near  $T_c$ , whereas an enhancement of the diffuse-scattering intensity is not observed in Rb-TCNQ, in accord with the first-order-like nature of the phase transition.

Such a difference in the phase transition in K-TCNQ and Rb-TCNQ may be attributed to the difference in the geometry of neighboring TCNQ molecules on the stack in the respective lattices, as described before. Various properties of the dimerized lattice depend sensitively on the transfer integral between TCNQ molecules within the same dimer unit (intradimer transfer,  $t_1$ ) and between molecules in the adjacent dimers (interdimer

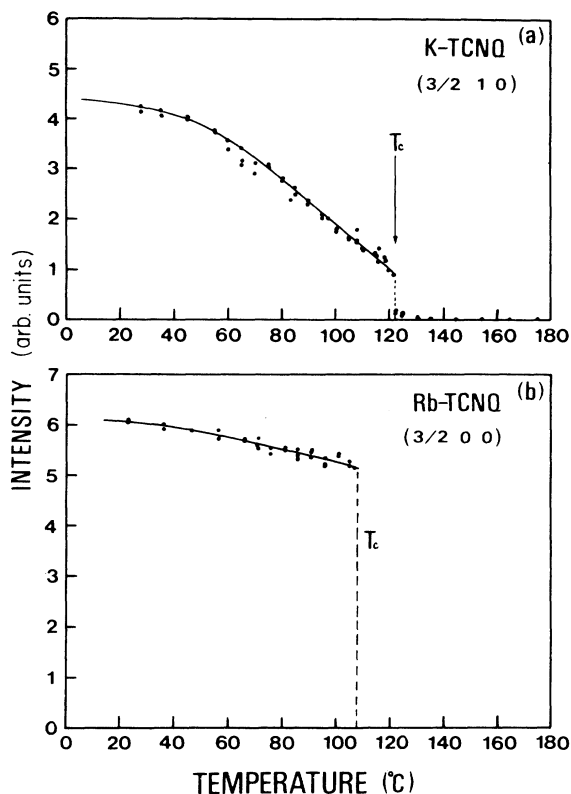


FIG. 1. Temperature dependence of the superlattice x-ray reflection intensity reported by Terauchi (taken from Ref. 5). (a) K-TCNQ and (b) Rb-TCNQ.

transfer,  $t_2$ ). In some TCNQ salts these important parameters have been calculated theoretically, for instance, in the recent linear combination of atomic orbitals (LCAO) calculation for methylethylmorpholinium (TCNQ)<sub>2</sub> and other TCNQ salts, by Smaalen and Kommandeur.<sup>27</sup> However, such an approach has not yet been taken with K-TCNQ and Rb-TCNQ. Therefore, in the present study we employed an empirical approach to the structural phase transitions in K-TCNQ and Rb-TCNQ. Observed phase features in the polarized reflection spectra have been quantitatively analyzed as much as possible to derive experimental information complementary to the previous x-ray data on the phase-transition mechanism.

### III. EXPERIMENTAL DETAILS

Single crystals of K-TCNQ and Rb-TCNQ were grown by the liquid-phase reaction process of the constituent cation ( $K^+$  or  $Rb^+$ ) and TCNQ<sup>-</sup> radical anion through diffusion in the acetonitrile solution at 15–20°C. As the starting materials, reagent-grade commercial powders of KI and RbI were used. For TCNQ, commercially available powders were not sufficiently pure, so they were purified by several sublimations. The diffusion growth of single crystals was made using the standard method. After the reaction within the acetonitrile solutions, which took about 20 d, needlelike single crystals were obtained. The typical sizes were about

$10 \times 1 \times 1 \text{ mm}^3$  for K-TCNQ and about  $8 \times 0.7 \times 0.7 \text{ mm}^3$  for Rb-TCNQ.

In the measurements of polarized reflection spectra, light from a halogen-tungsten incandescent lamp was used in the wavelength region of  $\lambda < 3 \mu\text{m}$ . In the longer-wavelength region ( $2.5 < \lambda < 5 \mu\text{m}$ ), a nichrome electric heater wire was also used. The light from these sources was focused by a concave mirror at the entrance slit of a 1000-mm grating monochromator (JASCO CT-100). The monochromatic light from the exit slit was passed through a polarizer, and was focused by a concave mirror on the specific surface of a single-crystal sample in a variable-temperature cryostat. Reflected light from the sample was focused by a concave mirror on a sensitive position of the detector. Suitable detectors were selected, depending on the wavelength region, from a photomultiplier tube (in the visible region), a PbS cell (held at room temperature or cooled to about 195 K by a dry-ice-ethanol refrigerant, in 1–3.5  $\mu\text{m}$ ), an Hg-Cd-Te photoconductive cell (cooled to about  $-60^\circ\text{C}$ , in 3–5  $\mu\text{m}$ ).

The samples were mounted in a glass cryostat having an optical window made of sapphire or BaF<sub>2</sub> plate. The sample temperature was controlled from 2 to about 420 K with an accuracy of 0.5 K. Precautions were taken to prevent the sample from thermal strain upon cooling. Needlelike single crystals of K-TCNQ or Rb-TCNQ were carefully fixed onto a metallic cold finger within the cryostat using a small amount of grease or silver paste. For the measurements at elevated temperatures, the sample was heated *in vacuo* to prevent oxidation.

When single-crystal samples of Rb-TCNQ were warmed up to about 400 K, macroscopic cracks were often found to be introduced within crystals after passing across the critical temperature of 381 K for the structural phase transition. But there was no serious effect of the cracks on the spectral features presented in the next section. The spectra were quite reproducible for repeated temperature changes across the phase-transition temperature. It is considered, therefore, that the crystal structure is not disturbed so much by the local disorders associated with the cracks.

### IV. EXPERIMENTAL RESULTS

The polarized reflection spectra of K-TCNQ and Rb-TCNQ crystals at 77 K are shown in Figs. 2(a) and 2(b). The upper and lower parts of either panel show the spectra for the polarized light with the electric vector parallel ( $E||a$ ) and perpendicular ( $E \perp a$ ), respectively, to the stacking axis ( $a$  axis). The spectra are composed of the following features: several broad bands in the visible region above 1.5 eV, a strong band observed only in the  $E||a$  spectra around 1.0–1.1 eV, and a very sharp peak in the infrared region. The structures in the visible region are assigned to the intramolecular electronic excitation bands in the TCNQ molecule. In K-TCNQ, the band at about 2.0 eV is predominantly polarized for  $E \perp a$ , while in Rb-TCNQ the structures around 2.0 eV have considerable intensity for  $E||a$ . These features can be explained by the directions of transition dipole moments for these intramolecular excitations. The moments lie on the molecu-

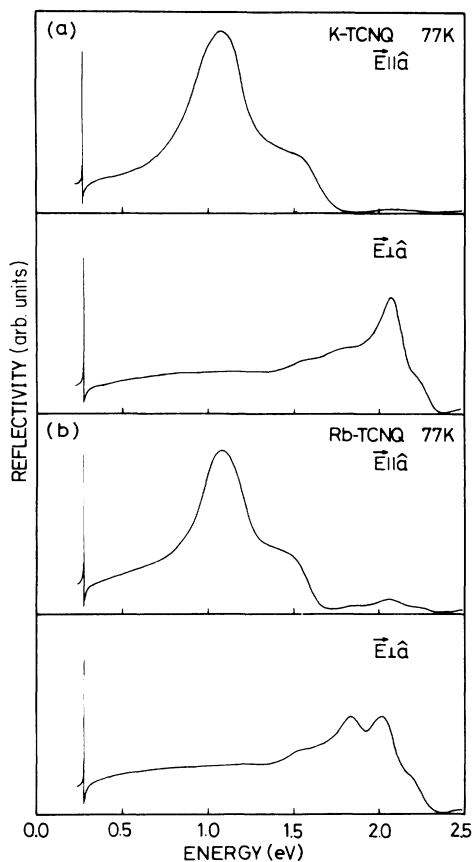


FIG. 2. Reflectivity spectra of single crystals of (a) K-TCNQ and (b) Rb-TCNQ at 77 K for polarized lights with  $E\parallel a$  and  $E\perp a$  ( $a$  being the stacking axis).

lar planes of TCNQ, which are nearly perpendicular to the  $a$  axis in K-TCNQ, but are considerably inclined to the  $a$  axis in Rb-TCNQ as described before. A prominent band observed in both K-TCNQ and Rb-TCNQ crystals around 1.1 eV is assigned to the CT excitation taking place between TCNQ molecules on the same stack, as evidenced by the predominant polarization along the stacking axis. The main CT band is accompanied by a shoulderlike structure at about 1.5 eV in either crystal. These features in the visible and near-infrared regions are essentially in agreement with the previous results reported by Yakushi *et al.*<sup>13,14</sup>

Sharp structures observed in the infrared region are assigned to the CN stretching mode of the TCNQ molecule. They are observed at almost the same energy, about 0.27 eV or 2200  $\text{cm}^{-1}$ , in both K-TCNQ and Rb-TCNQ, reflecting the localized nature of the molecular vibration. More detailed shapes of the CN stretching vibrational band in K-TCNQ and Rb-TCNQ are plotted in Fig. 3 at various temperatures below and above the respective phase-transition temperatures (395 K in K-TCNQ and 381 K in Rb-TCNQ). The solid and dotted curves represent the polarized components for  $E\parallel a$  and  $E\perp a$ , respectively. The spectra are plotted in  $\text{cm}^{-1}$  instead of eV as in Fig. 2, following the custom in the molecular vibra-

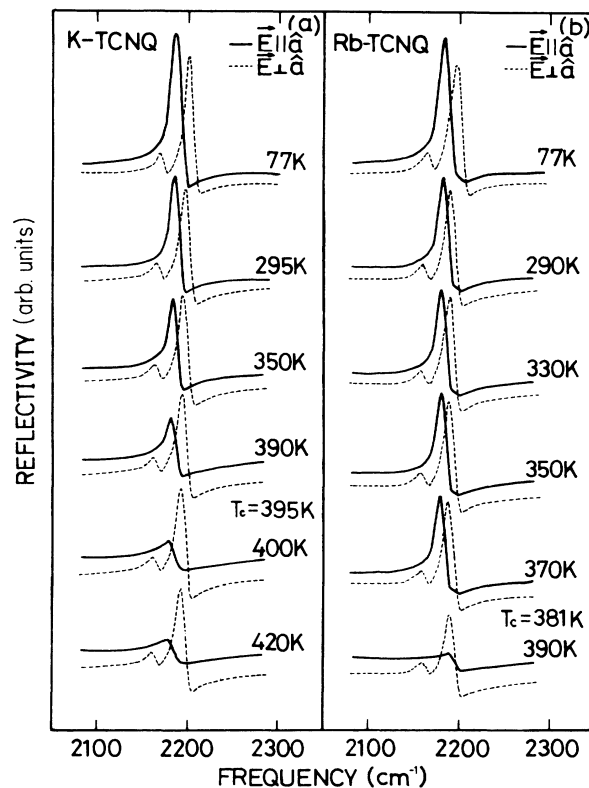


FIG. 3. Molecular structures of TCNQ and ( $a_g, b_{1u}, b_{2u}$ ) intramolecular vibration modes associated with the CN stretching vibrations.

tion spectroscopy. As seen, the spectra of K-TCNQ and Rb-TCNQ crystals are very similar in shape and frequency: In K-TCNQ, the  $E\parallel a$  spectra show a single peak at about 2186  $\text{cm}^{-1}$ , while the  $E\perp a$  spectra exhibit double peaks, the larger one at about 2200  $\text{cm}^{-1}$  and the smaller at about 2167  $\text{cm}^{-1}$  at 77 K. These three modes are associated with the CN stretching vibrations in TCNQ molecules. From the molecular spectroscopic data,<sup>17</sup> the 2186- $\text{cm}^{-1}$  ( $E\parallel a$ ) peak is assigned to the totally symmetric ( $a_g$ ) mode, while the 2200- and 2167- $\text{cm}^{-1}$  peaks in the  $E\perp a$  spectra are attributed to the  $b_{1u}$  and  $b_{2u}$  modes, respectively. A schematic illustration of the  $a_g$ ,  $b_{1u}$ , and  $b_{2u}$  modes are shown in Fig. 4. The corresponding peaks in the spectra of Rb-TCNQ are assigned to the same modes as those in K-TCNQ.

A remarkable point in the molecular vibration spectra is that the totally symmetric ( $a_g$ ) modes in either K-TCNQ and Rb-TCNQ crystals are observed at low temperatures with intensity comparable to the infrared-active  $b_{1u}$  and  $b_{2u}$  modes. In an isolated TCNQ molecule, the corresponding  $a_g$  mode is not infrared active, because of the presence of an inversion symmetry in the molecule (cf. Fig. 4). The same mode would be also inactive for optical excitation in K-TCNQ and Rb-TCNQ crystals, if the center of inversion symmetry is located at the center of gravity for each molecule in the regular stacks. Actually, this mode is strongly activated in either crystals at low

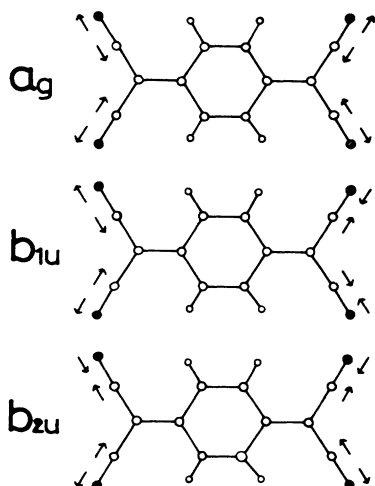


FIG. 4. Polarized reflectivity spectra due to the  $a_g, b_{1u}, b_{2u}$  CN stretching vibration bands in (a) K-TCNQ and (b) Rb-TCNQ.

temperatures because the inversion symmetry of each TCNQ molecule in the crystal disappears by dimeric molecular displacements, as discussed by several authors before.<sup>15,16,28</sup> Detailed discussions on this mechanism are given in the next section in terms of a simplified model.

The experimental information on thermal behavior of the dimerized lattice can be derived from the temperature dependence of the spectra shown in Fig. 3. When the temperature is raised above 300 K, the intensity of the  $a_g$  peak in K-TCNQ crystal is gradually decreased, whereas the intensities of the  $b_{1u}$  and  $b_{2u}$  peaks do not show appreciable change with temperature. Above  $T_c$  ( $=395$  K), the  $a_g$  peak is much weaker than the  $b_{1u}$  and  $b_{2u}$  peaks. The thermal effect on the  $a_g$  peak is even more drastic in the spectra of Rb-TCNQ. Spectral features are essentially unchanged up to about 370 K, except for a slight broadening of the respective structures. But, when temperature is raised further, the intensity of the  $a_g$  peak suddenly diminishes at about 380 K. In the  $E||a$  spectra at 390 K [the bottom curve in Fig. 3(b)], a weak structure is observed at about  $2192\text{ cm}^{-1}$ . However, this structure is not due to the residual  $a_g$  mode. It is identified with the weak  $E||a$  component of the intense  $b_{1u}$  band, which is predominantly polarized for  $E||a$ . In fact, the same structure is found as a slight hump in the  $E||a$  spectra below 370 K on the high-energy side of the  $a_g$  band. There is no detectable structure at all in the 390-K spectrum at the position (about  $2178\text{ cm}^{-1}$ ) where the intense  $a_g$  mode is observed up to about 370 K. Thus, one can conclude that the  $a_g$  mode which is strongly activated at low temperatures suddenly and completely disappears near the critical temperature,  $T_c = 381$  K, for the structural phase transition.

In contrast with the discontinuous change of the  $a_g$  band in Rb-TCNQ crystal, the thermal change of the  $a_g$  peak in K-TCNQ crystal is not so drastic at the phase transition temperature  $T_c$  ( $=395$  K). This is in agree-

ment with the result reported before by Iqbal *et al.*<sup>17</sup> on polycrystalline K-TCNQ, except for the following point. The intensity of the  $a_g$  peak is gradually decreased with increasing temperature, but even above  $T_c$  the  $E||a$  spectra show a weak peak at the same position where the strong peak is observed below  $T_c$ . This peak cannot be identified with the component of the  $b_{1u}$  band as in the case of Rb-TCNQ crystal above  $T_c$ , but is evidently assigned to the residual  $a_g$  band. Iqbal *et al.*<sup>17</sup> have concluded that the  $a_g$  band completely disappears at  $T_c$  from measurements on the unpolarized powder spectra. However, it is quite difficult to distinguish the weak residual  $a_g$  peak from the intense  $b_{1u}$  band as seen in Fig. 3. The polarized spectra presently observed clearly demonstrate that the  $a_g$  mode in K-TCNQ remains still infrared active above  $T_c = 395$  K, though the intensity is considerably weakened. Quantitative analysis of the  $a_g$  band in K-TCNQ and Rb-TCNQ crystals are given in the next section.

We next turn our attention to the temperature dependence of the CT bands in the near-infrared region (0.8–1.5 eV). Reflecting the quasi-one-dimensional character of the CT excitation, the spectra are predominantly polarized along the stacking axis, as seen in Fig. 2. The temperature changes of the CT bands in K-TCNQ and Rb-TCNQ crystals are shown in Fig. 5 at various temperatures above and below  $T_c$ . Only the  $E||a$  polarized spectra are presented. The spectra of either crystals at 2 K (shown at the top) consist of two bands, the strong main reflection band (*A*) at about 1.1 eV and the subsidiary band (*B*) around 1.5 eV. The *A* and *B* bands are both absent in the absorption spectra of isolated TCNQ molecules, and can be assigned to the intermolecular electronic CT excitations along the TCNQ<sup>-</sup> stack. The *B* band has been assigned by Yakushi *et al.*<sup>13,14</sup> to the band-edge transition of a free-electron-hole-pair excitation. However, this interpretation seems to be inconsistent with the exper-

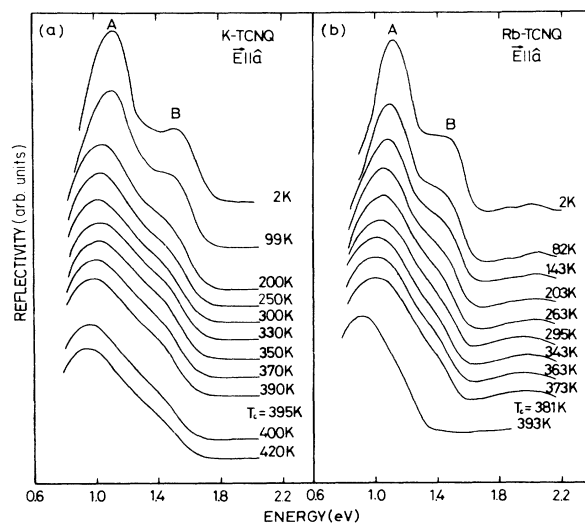


FIG. 5. Polarized reflection spectra due to the charge-transfer excitons in (a) K-TCNQ and (b) Rb-TCNQ. Only the  $E||a$  spectra are presented.

imental results described below. An alternative model for the origin of the *B* band is presented in the next section.

When temperature is raised from 2 K, the *A* band shows an appreciable broadening and a slight red shift with increasing temperature, but the integrated intensity of the band remains almost unchanged up to the highest temperature investigated (420 K for K-TCNQ and 393 K for Rb-TCNQ). Contrary to this, the intensity of the *B* band is steadily decreased with increasing temperature and finally becomes barely observable near  $T_c$ . Like the case of intramolecular  $a_g$  bands, there is a difference between the thermal behaviors of the CT band in K-TCNQ and Rb-TCNQ crystals. In K-TCNQ, a slight hump remains observable at about 1.5 eV above  $T_c$ , while in Rb-TCNQ there is no observable structure at all on the high-energy side of the *A* band when temperature is raised above  $T_c$ .

## V. DISCUSSION

### A. Simplified picture of CT excitations and $a_g$ molecular vibrations in dimerized metal-TCNQ crystals

Before proceeding to a quantitative analysis of the experimental results presented in the preceding section, we consider a simplified picture for the CT excitons and optically activated  $a_g$  intramolecular vibrations in dimerized K-TCNQ and Rb-TCNQ crystals. Let us first examine the case of undimerized regular stacks of TCNQ<sup>-</sup> molecules. In the quasi-one-dimensional stacks of K-TCNQ and Rb-TCNQ crystals, the CT excitations are conceived, in a simple model, as an electron-transfer process between two TCNQ molecules on the same stack in such a way as  $\text{TCNQ}^- + \text{TCNQ}^- \rightarrow \text{TCNQ}^0 + \text{TCNQ}^{2-}$ . In the regularly stacked crystal, the electron transfers from a given TCNQ<sup>-</sup> molecule can occur in either directions of a given TCNQ<sup>-</sup> molecule with the same excitation energy. In the presence of the electron-transfer interaction between molecules on the stack, the lowest CT excitons are composed of an even-parity CT state ( $|e\text{-CT}\rangle$ ) and an odd-parity CT state ( $|o\text{-CT}\rangle$ ), which are formed by the linear combinations of the degenerate CT excitations in the backward and forward directions of the central TCNQ<sup>-</sup> molecule. Of these two CT excitons, the  $|e\text{-CT}\rangle$  exciton is located above the  $|o\text{-CT}\rangle$  exciton, as shown in Fig. 6(a), because of the mixing effect between the former exciton and the ground state ( $|G\rangle$ ) through the electron-transfer interaction. The optical transition from the ground state is permitted only to the  $|o\text{-CT}\rangle$  exciton in the regular stacks of the undimerized crystal.

When dimeric displacement takes place in the TCNQ columns, the inversion symmetry around each molecule in the stack is lifted and the unit-cell length along the stack is doubled. Therefore, the dispersion curve of the CT exciton is folded back at  $k = \pi/2a$  ( $a$  being the intermolecular spacing in the regular stack). We then have two additional zone-center excited states. Of these two states, only the higher one associated with the  $|e\text{-CT}\rangle$  state becomes weakly optically active, as understood easily by considering the symmetry of these excited states. This will lead to

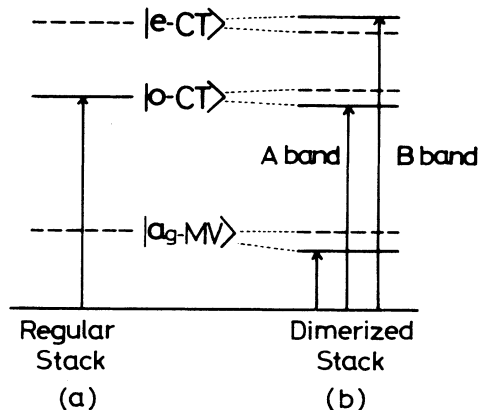


FIG. 6. A simplified model for optical excitations in the one-dimensional column of TCNQ molecules. (a) Regular stack and (b) dimerized stack. Levels of the  $a_g$  molecular vibration  $|a_g\text{-MV}\rangle$  and the even, odd-CT excitons  $|o,e\text{-CT}\rangle$  are schematically shown. Arrows indicate dipole-allowed transitions.

the appearance of a weak absorption (or reflection) peak on the high-energy side of the main CT band (corresponding to the  $|o\text{-CT}\rangle$  state) when the crystal is subject to a dimeric molecular displacement. From discussions described later, we assign the reflection peaks *A* and *B* in the low-temperature spectra in Fig. 5 to the optical excitations of the  $|o\text{-CT}\rangle$  and  $|e\text{-CT}\rangle$  excitons, as indicated in Fig. 6, in the dimerized lattice. The dimerization of TCNQ columns also gives rise to the optical activation of the totally symmetric ( $a_g$ ) intramolecular vibrations of TCNQ molecules, particularly the  $a_g$  CN stretching mode in the present case. This mechanism, called the electron molecular vibration (EMV) coupling effect, has been dealt with in detail in the literature.<sup>15,16,20,28,29</sup> The physical picture for it may be described as follows. Let us consider the molecular vibrational phonon associated with a particular intramolecular  $a_g$  mode. In the regularly stacked molecular columns, the zone-center mode at  $k=0$  corresponds to the vibrational state in which all molecules on the stack are vibrating in phase, while in the zone-edge mode at  $k=\pi/a$  molecules on the alternating sites are vibrating 90° out of phase. The  $k=0$  phonon is not optically active from symmetry in this case.

When the molecular stack is dimerized, the dispersion curve of the phonon is folded back at  $k = \pi/2a$ , just as the CT exciton is. Then we have two zone-center modes of molecular vibration, the one with two adjacent molecules in the dimer unit vibrating in phase and the other with two molecules vibrating 90° out of phase. It is not difficult to understand that while the former mode remains optically inactive, the latter mode induces an oscillating electric dipole moment within the dimer unit because of an uneven distribution of the valence electrons on the two TCNQ molecules by the out-of-phase  $a_g$  vibrations in them. The magnitude of this induced dipole moment is strongly dependent on the amplitude of electron intramolecular vibration coupling and on the difference in the intradimer and interdimer electron-transfer interactions ( $t_1, t_2$ ),

which is supposed to be nearly proportional to the dimeric molecular displacement in the case of weak dimerization. This mode can be resonantly excited by light with the electric vector in parallel to the stacking axis through the electromagnetic coupling between the induced electric dipole moment in the dimers and the electric field in the light. Appearance of prominent absorption (or reflection) bands of some  $a_g$  intramolecular vibration modes in the dimerized phase of several CT complex crystals is attributable to the aforementioned mechanism. Its remarkable intensity, as seen in Fig. 4, is directly derived from the higher-lying strong CT excitation band. This is evidenced by the complete polarization of the  $a_g$  bands (solid curves in Fig. 4) along the  $a$  axis in both K-TCNQ and Rb-TCNQ crystals.

A simple picture of CT excitons and  $a_g$  (CN stretching) intramolecular vibrations is illustrated in Fig. 6 for undimerized and dimerized quasi-one-dimensional stacks of TCNQ molecules. In the following discussion, we try to derive experimental information on the quantitative aspect of the model presented in Fig. 6.

#### B. Temperature dependence of $a_g$ CN stretching vibration bands

The shapes of reflection spectra due to the CN stretching vibrations in TCNQ shown in Fig. 4 exhibit characteristic dispersions expected for a classical Lorentz oscillator model. To analyze the temperature-dependent features of the  $a_g$  bands (solid curves in Fig. 4), we have tried to apply a simple isolated Lorentz oscillator model, which is represented by a complex dielectric function

$$\tilde{\epsilon}(\omega) = \epsilon_\infty + \frac{4\pi\omega_0^2\beta}{\omega_0^2 - \omega^2 - j\Gamma\omega} \quad (1)$$

Here,  $\omega_0$  is the resonance frequency,  $\beta$  the polarizability proportional to the intensity of the  $a_g$  band, and  $\Gamma$  the width of the  $a_g$  band. The contribution of the background polarization is expressed by a frequency-independent constant  $\epsilon_\infty$ . Theoretical reflectivity spectra were calculated from the real and imaginary parts of  $\tilde{\epsilon}$  for a given set of adjustable parameters,  $\epsilon_\infty$ ,  $\omega_0$ ,  $\Gamma$ , and  $\beta$ . As a result of a least-squares-fitting procedure, the values for these parameters have been evaluated for the respective spectra in Fig. 4 at various temperatures. For the spectra in Rb-TCNQ, the presence of the weak  $b_{2u}$  band on the high-energy side of the  $a_g$  band has also been taken into account. As the intensity of the  $b_{2u}$  ( $E||a$ ) band is proportional to the intensity of corresponding  $E||a$  spectra, one can eliminate the contribution of the overlapping  $b_{2u}$  ( $E||a$ ) band by subtracting a constant fraction of the  $b_{2u}$  ( $E||a$ ) spectra observed at the same temperature. The agreement between the experimental and calculated spectra was found to be very good in both K-TCNQ and Rb-TCNQ crystals.

The values for  $\beta$  and  $\Gamma$  of the  $a_g$  bands for K-TCNQ and Rb-TCNQ are plotted in Fig. 7 against temperature. The strength  $\beta$  of the  $a_g$  bands in either crystals show characteristic temperature dependence; a gradual decrease with increasing temperature below  $T_c$  in K-TCNQ and a steep drop to zero at  $T_c$  in Rb-TCNQ. Overall behaviors

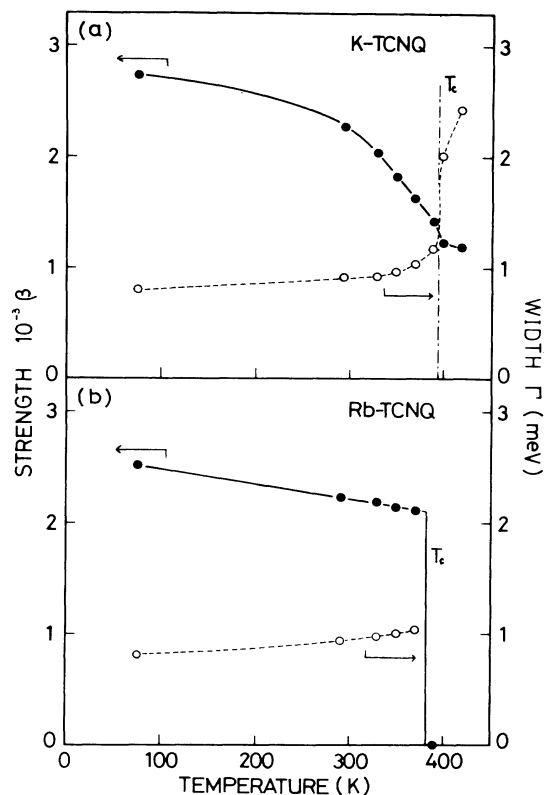


FIG. 7. Temperature dependence of absorption strength  $\beta$  (solid circles) and linewidth  $\Gamma$  (open circles) of the  $a_g$  CN stretching intramolecular vibration bands. (a) K-TCNQ and (b) Rb-TCNQ.

are quite similar to the critical changes in the x-ray-diffraction intensities of the respective crystals shown in Fig. 1. In the case of K-TCNQ, however, there is a notable difference between the thermal behaviors of the  $a_g$  band and of the x-ray data: The  $a_g$  band does not disappear at  $T_c$ , but retains a considerable intensity above  $T_c$ , whereas the x-ray result shows a sudden drop of the intensity essentially to zero at  $T_c$ .

Looking at the temperature dependence of the width  $\Gamma$  for the  $a_g$  band in either crystal, one finds that there is a significant difference between the results in K-TCNQ and Rb-TCNQ. In Rb-TCNQ, the experimental values for  $\Gamma$  are nearly constant over a wide temperature range below  $T_c$ , until the  $a_g$  band suddenly disappears at  $T_c$ . In K-TCNQ,  $\Gamma$  is nearly constant below  $T_c$  and shows a sudden jump at  $T_c$  to a value which is more than twice as large as those below  $T_c$ . This implies that the  $a_g$  band suffers a considerable broadening at  $T_c$ . In contrast, the intensity  $\beta$  does not show such a drastic change at  $T_c$ . These observations suggest that the dimeric distortion in K-TCNQ remains to be finite even above  $T_c$ . Furthermore, a sharp rise of  $\Gamma$  at  $T_c$  implies that the dimerized lattice is in a state of rapid dynamical fluctuation. Such a fluctuating dimeric displacement of TCNQ molecules, if any, will be not able to be detected by the x-ray-diffraction study, since it measures a three-

dimensional space-averaged displacement in the lattice. To detect the critical fluctuation at the phase transition, one has to measure diffuse x-ray scattering. In fact, an experimental result on the  $(\frac{3}{2} 1 0)$  diffuse scattering intensity in K-TCNQ clearly indicates an appearance of fairly large critical fluctuation in the lattice above  $T_c$ .<sup>5</sup> On the other hand, there is no detectable diffuse x-ray scattering in Rb-TCNQ at  $T_c$ , indicating a first-order transition from a statically dimerized lattice to a regularly stacked lattice without a critical fluctuation.<sup>5</sup> This is consistent with the results of the present optical study.

### C. Temperature dependence of CT bands

The CT bands in the near-infrared region consist of two broad structures, *A* and *B*, in either K-TCNQ and Rb-TCNQ crystals at low temperatures. Because of an appreciable overlapping between the two reflection bands, it is hard to make a quantitative estimation of intensities and half-widths of the respective bands directly from the observed reflection spectra. In order to derive reliable information on the thermal behaviors of the CT bands, we have applied a least-squares-fit procedure, similar to that applied to the  $a_g$  molecular vibrational bands, by assuming a model dielectric function given by

$$\tilde{\epsilon}(\omega) = \epsilon_\infty + \sum_{i=A,B} \frac{S_i}{\omega_i^2 - \omega^2 - j\Gamma_i\omega}$$

Here,  $S_i = 4\pi\omega_i^2\beta_i$  ( $i = A, B$ ) is defined as the intensity of *A* or *B* band with the resonance frequency  $\omega_i$  and the bandwidth  $\Gamma_i$ . From the best-fit procedure, values for these adjustable parameters have been determined at various temperatures. As the *B*-exciton band is considerably weak and broad, the parameters for the *B* exciton include some ambiguity at high temperatures. Except for this point, the agreement between the calculated and experimental reflectivity spectra was fairly good in both K-TCNQ and Rb-TCNQ crystals.

A conspicuous feature in the temperature dependence of CT bands shown in Fig. 5 is that the intensity of the *B* band is strongly dependent on temperature, whereas the integrated intensity of the *A* band is nearly constant up to fairly high temperatures in either crystal, as demonstrated in Fig. 8. Here the ratio  $S_B/S_A$  derived from the above-mentioned procedure is plotted as a function of temperature. In both crystals, the ratio decreases steadily as temperature is increased to  $T_c$ . The *B* band in Rb-TCNQ seems to disappear rather abruptly at  $T_c$ , but that in K-TCNQ retains an observable intensity above  $T_c$ . This is in accord with the thermal behavior of the  $a_g$  molecular vibration band. The dynamical property of the CT excitons also manifests itself in the temperature dependence of the bandwidth  $\Gamma_{A,B}$  shown in Fig. 9. The experimental points for  $\Gamma_A$  in K-TCNQ show a remarkable increase near  $T_c$ , though not so conspicuous as observed in the  $a_g$  vibration bands (Fig. 7). This is considered attributable to the effect of critical fluctuation in TCNQ columns upon CT excitation.

From the experimental results presented above, it is evident that the subsidiary CT band (the *B* band) is directly related with the dimeric molecular displacement

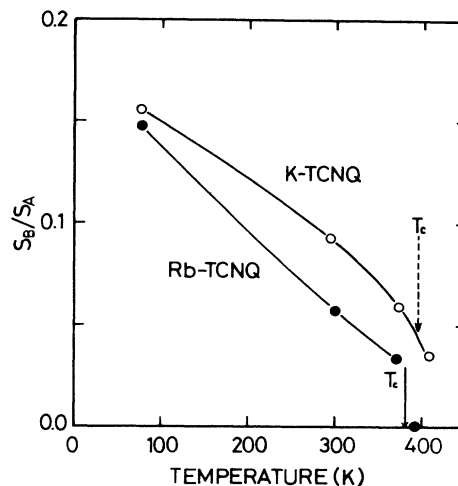


FIG. 8. Temperature dependence of relative absorption intensities  $S_B/S_A$  for the main (*A*) and subsidiary (*B*) CT exciton bands in K-TCNQ (open circles) and Rb-TCNQ (solid circles).

in both K-TCNQ and Rb-TCNQ crystals. Similar structure has been also observed in the reflection spectra of TTF-*p*-chloranil crystal<sup>30</sup> in the low-temperature phase in which the lattice is dimerized. We therefore consider that this band ought to be assigned to the symmetry-

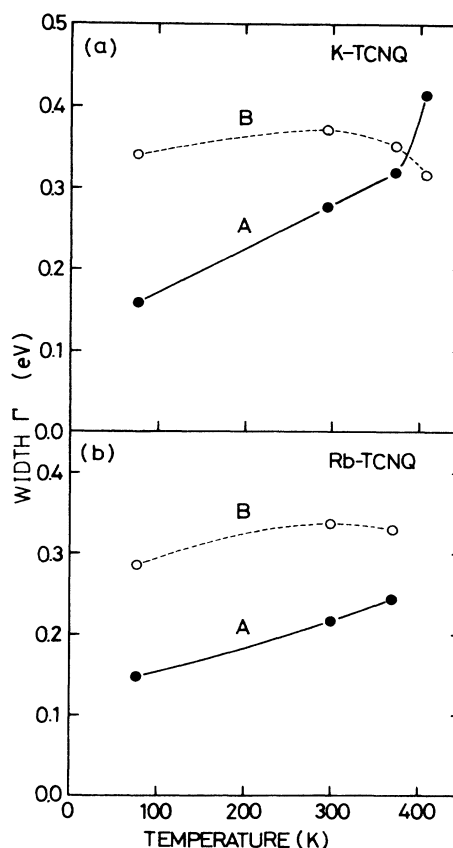


FIG. 9. Temperature dependence of linewidth  $\Gamma$  for the main (*A*) and subsidiary (*B*) CT exciton bands in K, Rb-TCNQ.



perturbed even-parity CT exciton ( $|e\text{-CT}\rangle$ ), as depicted in Fig. 6(b), rather than the interband absorption edge, as suggested by Yakushi *et al.*<sup>13,14</sup>

#### D. A picture of phase transition in K,Rb-TCNQ from optical study

In accord with the previous x-ray data,<sup>5</sup> the present optical study has demonstrated that the dimeric distortion in Rb-TCNQ shows a first-order-like discontinuous change at  $T_c$ , while the dimerization in K-TCNQ shows a gradual change below  $T_c$  and an appreciable fluctuation above  $T_c$ . Such a notable difference in the thermal behavior of structural transitions in K-TCNQ and Rb-TCNQ crystals may be primarily attributed to the difference in the intermolecular electron-transfer interaction, which is sensitively dependent on the molecular geometry in the crystal structure. In the following discussion, a qualitative picture of the phase transitions in K,Rb-TCNQ is discussed on the basis of the present optical data in conjunction with the previous information from the x-ray measurements.

The infrared reflection bands (the  $a_g$  CN stretching vibration bands) are due to the electric dipole moment induced by the coupling of dimeric displacement and the intramolecular  $a_g$  vibration. Reflecting such a local nature of the optical response, the intensity of these bands,  $\beta$ , is predominantly determined by the amplitude of the local dimeric displacement. Thus their bandwidth is considered to be affected by the temporal fluctuation of displacement in addition to the natural width below  $T_c$ . To account for the sharp increase of  $\Gamma$  in K-TCNQ around  $T_c$ , one can consider two possible causes: a fluctuation in the amplitude of dimeric displacement and a fluctuation in the frequency of EMV-activated infrared vibration. Actually, these two causes are closely related to each other. Supposedly, the latter effect is relatively small, and the sharp increase of  $\Gamma$  observed around  $T_c$  may be primarily attributed to the change in correlation time for the dimeric displacement. From the increment of  $\Gamma$  in K-TCNQ by about 1 meV at  $T_c$ , the correlation time is evaluated to be about  $10^{-11}$  s. On the other hand, the intensity and linewidth of the forbidden x-ray-diffraction line shown in Fig. 1 are determined by the spatial average of the squared molecular displacement and its correlation length, which provides information on the long-range order of molecular dimerization. The x-ray data on K-TCNQ [Fig. 1(a)] demonstrate that the three-dimensional long-range order of dimeric displacement disappears at  $T_c$ . However, the nonvanishing intensity of the  $a_g$  band [Fig. 7(a)] above  $T_c$  indicates that the local dimerization still exists on the quasi-one-dimensional TCNQ columns even above  $T_c$ . This local dimeric displacement is considered to be rapidly fluctuating with a correlation time of the order of  $10^{-11}$  s, as mentioned above.

From these observations, we present the following picture for the dynamical nature of the phase transition in K-TCNQ: At sufficiently low temperatures, the dimerized lattice has a three-dimensional static order both on the molecular stacks and between the columns. As the temperature is raised, the intercolumn correlation is grad-

ually decreased, presumably due to a thermal excitation of mobile solitonlike defects on the dimerized columns. At  $T_c$ , the intercolumn correlation of dimerization is completely lost because of independent fluctuation of dimeric displacements on different columns. Yet, it is supposed that there exist local regions (domains) on the respective columns in which the dimeric displacements persist even above  $T_c$ . This implies that the one-dimensional column of TCNQ is subject to a spin-Peierls-like distortion still above  $T_c$ . Similar behavior has been also reported on Na-TCNQ and Rb-TCNQ(II) crystals from infrared spectra of powder samples.<sup>18</sup>

The dimeric distortion in the lattice is also related to the behavior of the magnetic susceptibility  $\chi$  at the phase transition. The temperature variation of  $\chi$  of K-TCNQ has been analyzed by Lepine *et al.*<sup>7</sup> in terms of a Heisenberg Hamiltonian. According to their results, the behavior of  $\chi$  above  $T_c$  cannot be explained by a linear Heisenberg Hamiltonian assuming a constant antiferromagnetic exchange  $J$ . They have attributed the difference between the experimental and theoretical values of  $\chi$  to the temperature dependence of  $J$ . However, according to the present result the lattice of the K-TCNQ crystal is not regular above  $T_c$ , so it is not appropriate to assume a single  $J$ , as has been assumed by these authors. It is supposed that the discrepancy between the theoretical and experimental  $\chi$  values above  $T_c$  may be attributed to a pseudomagnetic gap which is caused by the dynamically fluctuating displacement in the TCNQ columns above  $T_c$ .

In contrast to the dynamical behavior in K-TCNQ, the phase transition in Rb-TCNQ shows a typical first-order-like feature in both optical and x-ray data at  $T_c$ . This indicates that the local dimeric displacement disappears simultaneously with the vanishing of three-dimensional order at  $T_c$ . In this sense, the phase transition in Rb-TCNQ is predominantly structural in character. The spin-Peierls mechanism is considered to play only a secondary role, that of assisting this transition, as suggested by Lepine.<sup>9</sup>

In conclusion, it has been demonstrated that the measurements of  $a_g$  intramolecular vibration bands on single crystals are not only useful for detecting the lattice dimerization, as was previously done on unpolarized powder spectra, but also capable of providing quantitative information on the molecular displacement in complement of the x-ray data.<sup>5</sup> From a spectral shape analysis of the polarized spectra, one can investigate the local behavior of molecular displacements which are not accessible by x-ray measurement.

#### ACKNOWLEDGMENTS

The authors are grateful to Professor G. Saito, University of Tokyo, for valuable advice on sample preparation, and to Dr. N. Nagaosa, University of Tokyo, and Professor H. Yamada, Kwansai Gakuin University, for enlightening discussions. Part of this work was supported by a Grant-in-Aid from the Special Research Project on Properties of Molecular Assemblies from the Ministry of Education, Science and Culture, Japan.

- \*Present address: Department of Physics, University of Tokyo Bunkyo, Tokyo 113, Japan.
- <sup>1</sup>For a review, see H. Endres, in *Extended Linear Chain Compounds*, edited by J. S. Miller (Plenum, New York, 1983), Vol. 3, p. 263.
- <sup>2</sup>J. G. Vegter, T. Hibma, and J. Kommandeur, *Chem. Phys. Lett.* **3**, 427 (1969).
- <sup>3</sup>A. Hoekstra, T. Spoelder, and A. Vos, *Acta Crystallogr. Sect. B* **28**, 14 (1972).
- <sup>4</sup>N. Sakai, I. Shirovani, and S. Minomura, *Bull. Chem. Soc. Jpn.* **45**, 3321 (1972).
- <sup>5</sup>H. Terauchi, *Phys. Rev. B* **17**, 2446 (1978).
- <sup>6</sup>M. Konno, T. Ishii, and Y. Saito, *Acta Crystallogr. Sect. B* **33**, 763 (1977).
- <sup>7</sup>Y. Lépine, A. Caillé, and V. Larochelle, *Phys. Rev. B* **18**, 3585 (1978).
- <sup>8</sup>Y. Takaoka and K. Motizuki, *J. Phys. Soc. Jpn.* **47**, 1752 (1979).
- <sup>9</sup>Y. Lépine, *Phys. Rev. B* **28**, 2659 (1983).
- <sup>10</sup>S. K. Khanna, A. A. Bright, A. F. Garito, and A. J. Heeger, *Phys. Rev. B* **10**, 2139 (1974).
- <sup>11</sup>D. B. Tanner, C. S. Jacobson, A. A. Bright, and A. J. Heeger, *Phys. Rev. B* **16**, 3283 (1977).
- <sup>12</sup>G. R. Anderson and J. P. Devlin, *J. Phys. Chem.* **79**, 1100 (1975).
- <sup>13</sup>K. Yakushi, T. Kusaka, and H. Kuroda, *Chem. Phys. Lett.* **68**, 139 (1979).
- <sup>14</sup>K. Yakushi, S. Miyajima, T. Kusaka, and H. Kuroda, *Chem. Phys. Lett.* **114**, 168 (1985).
- <sup>15</sup>M. J. Rice, *Solid State Commun.* **31**, 93 (1979).
- <sup>16</sup>A. Painelli and A. Girlando, *J. Chem. Phys.* **84**, 5655 (1986).
- <sup>17</sup>Z. Iqbal, C. W. Christoe, and D. K. Dawson, *J. Chem. Phys.* **63**, 4485 (1975).
- <sup>18</sup>R. Bozio and C. Pecile, *J. Chem. Phys.* **67**, 3864 (1977).
- <sup>19</sup>S. Etemad, *Phys. Rev. B* **24**, 4959 (1981).
- <sup>20</sup>M. J. Rice, V. M. Yartsev, and C. S. Jacobsen, *Phys. Rev. B* **21**, 3437 (1980).
- <sup>21</sup>A. Girlando, F. Marzola, C. Pecile, and J. B. Torrance, *J. Chem. Phys.* **79**, 1075 (1983).
- <sup>22</sup>A. Girlando, A. Painelli, and C. Pecile, *Mol. Cryst. Liq. Cryst.* **112**, 325 (1984).
- <sup>23</sup>A. Girlando, A. Painelli, and C. Pecile, *Mol. Cryst. Liq. Cryst.* **120**, 17 (1985).
- <sup>24</sup>Y. Tokura, Y. Kaneko, H. Okamoto, S. Tanuma, T. Koda, T. Mitani, and G. Saito, *Mol. Cryst. Liq. Cryst.* **125**, 71 (1985).
- <sup>25</sup>M. Meneghetti, A. Girlando, and C. Pecile, *J. Chem. Phys.* **83**, 3134 (1985).
- <sup>26</sup>Y. Tokura, H. Okamoto, T. Koda, T. Mitani, and G. Saito, *Solid State Commun.* **57**, 607 (1986).
- <sup>27</sup>S. V. Smaalen and J. Kommandeur, *Phys. Rev. B* **31**, 8056 (1985).
- <sup>28</sup>M. J. Rice, N. O. Lipari, and S. Strässler, *Phys. Rev. Lett.* **39**, 1359 (1977).
- <sup>29</sup>A. Girlando, R. Bozio, and C. Pecile, *Phys. Rev. B* **26**, 2306 (1982).
- <sup>30</sup>Y. Tokura, T. Koda, T. Mitani, and G. Saito, *Solid State Commun.* **43**, 757 (1982).